Subsolidus phase relations in the $CaCO_3$–$MgCO_3$ system predicted from the excess enthalpies of supercell structures with single and double defects

Victor L. Vinograd*
Institute of Geosciences, University of Frankfurt, Altenhoeferallee 1, 60438 Frankfurt a.M., Germany

Marcel H. F. Sluiter
Department of Materials Science, Delft University of Technology, Mekelweg 2, 2628 CD, Delft, The Netherlands

Björn Winkler
Institute of Geosciences, University of Frankfurt, Altenhoeferallee 1, 60438 Frankfurt a.M., Germany
(Received 10 November 2008; revised manuscript received 27 January 2009; published 5 March 2009)

The thermodynamic mixing properties of a binary $(A_xB_{1-x})R$ solid solution are evaluated from the enthalpies of supercell structures $A_{m-2}B_2R_m$ and $B_{m-2}A_2R_m$, where m is the number of the exchangeable sites in the supercell. The excess enthalpies of these structures are converted into concentration-dependent pairwise effective cluster interactions J_n, i.e., the enthalpies of the intracrystalline reactions $AA+BB \rightleftharpoons 2AB$ acting at the n-neighbor distance within the supercell. The pairwise interactions calculated in this way for all possible distances within $3\times3\times1$ supercells of $R\bar{3}c$ calcite and magnesite ($m=54$) are combined to form an effective Ising-type Hamiltonian from which temperature-dependent enthalpies, entropies, and free energies of mixing are evaluated with the Monte Carlo method. The calculated phase diagram with two miscibility gaps separated by a field of stability of the $R\bar{3}$ dolomite phase is in good agreement with available experimental data, thereby showing that the existence of the intermediate ordered compound can be predicted from the analysis of the supercell structures whose compositions approach the diluted limits.

DOI: 10.1103/PhysRevB.79.104201 PACS number(s): 64.60.De, 64.70.qd, 64.75.Nx

I. INTRODUCTION

Modern approaches to modeling of solid solutions rely on the assumption that the thermodynamic effects of mixing and ordering can be predicted by studying the excess enthalpies of supercell structures with differently arranged exchangeable atoms. To reflect the most important ordering interactions, the supercell should be sufficiently large. This brings about the necessity of permuting a huge number of possible configurational states. Since only a limited set of such states can practically be tested, the simulation procedures employ interpolation methods which permit the excess enthalpy of a supercell with any configuration of the exchangeable atoms to be expressed through the enthalpies of a few explicitly sampled structures. In the method of the cluster expansion[1–3] this is achieved via the calculation of the effective cluster interactions (ECIs)—the locally defined energetic parameters, which after scaling by occurrence frequencies of the clusters give the value of the excess enthalpy. The ECIs can be calculated from the enthalpies of the sampled structures by solving a system of linear equations, provided that these structures correspond to different arrangements of the exchangeable atoms within the supercell.

The next important task of the simulation procedure is to extrapolate the excess properties of the supercell to a hypercell, i.e., a supercell whose properties approach that of an infinitely large system. This is achieved by expanding the supercell size so that several thousands of the exchangeable sites are included. The important condition for this extrapolation is that the ECIs converge fast with the increase in the separation between the points included in the clusters. This ensures that the hypercell has the same ground states as the supercell. Since the enthalpy of any possible configuration within the hypercell can be quickly calculated as a function of the ECIs and the cluster occurrence frequencies, the thermal averages of any relevant thermodynamic function can be obtained with a Monte Carlo algorithm.

In recent years this methodology has been applied to a large number of solid solutions, such as alloys, minerals, and ceramics. Different symmetries and chemical compositions of the studied materials dictated the use of different strategies of selecting the structures within the supercell which are to be included in the cluster expansion. In the studies of alloys and other solid solutions which crystallize in high-symmetry structures, such as fcc or bcc,[1,4–12] the sampled structures were often selected in analogy with ordered phases which typically appear as ground states in experimentally studied alloys. Using these structures is very convenient because true ground states are likely to be included in the basis set and thus the model is bound to be correct at least in the low-temperature limit. High symmetry of the basis structures and their relatively small size unit cells make the task of the enthalpy calculation tractable with *ab initio* methods. The development of the ATAT package[13] has permitted optimization of the selection of the basic clusters so that the best performance of the cluster expansion is achieved with minimum sizes of supercell structures.

On the other hand, in studies of minerals one is generally confronted with low-symmetry structures. The structural complexity and diversity of these materials prohibits a straightforward enumeration of possible ordered states. In contrast to alloys, where the unit cell is composed of the exchangeable atoms solely, minerals often contain extra "inactive" elements, e.g., O, Si, Al, and C, which increase the

 ©2009 The American Physical Society

system size. Typically one is concerned with ordering and mixing of cations of different metals which rest within an "inert" matrix built by anion complexes such as SiO_4^{4-}, AlO_6^{9-}, or CO_3^{2-}. The low symmetry and the chemical complexity typically imply a large unit cell, where the mixing occurs within a specific sublattice (Wyckoff position). For example, in grossular pyrope garnet, $Ca_3Al_2Si_3O_{12}$-$Mg_3Al_2Si_3O_{12}$, Ca and Mg are mixed over 24 out of the total number of 160 sites.[14] In such a case the approach based on ordered structures offers little advantage because the ordering affects just a small part of the structure and cannot significantly reduce the supercell size. At the same time, when interactions between exchangeable atoms in minerals are mediated by the "extra" elements, the role of many-body cluster interactions is likely to be small. The majority of the recent studies concerned with order/disorder and mixing phenomena in minerals[14–24] have therefore considered pairwise ECIs only. Since in large supercells a large number of different pair ECIs can be included in the expansion, it was usually possible to achieve reasonably accurate fits to the excess enthalpies of the sampled structures. Most of the above-mentioned studies were based on force-field models, while the sets of the basis structures were generated randomly. A typical study considered a few hundred structures of different compositions within a supercell containing 20–40 exchangeable sites.

This approach has two main drawbacks. First, the random choice of the basis structures introduces arbitrariness, as a different set of randomly selected structures will result in a different set of ECIs. Second, the use of hundreds of such structures does not allow consideration of *ab initio* calculations as a plausible alternative.

To overcome the difficulty of applying first-principles calculations in low-symmetry cases, here we employ a fully deterministic method which is based on the notion that the pairwise interactions in diluted limits can be evaluated from the excess enthalpies of supercell structures prepared from pure end members by substituting pairs of the exchangeable atoms with atoms of the other sort. The number of the required structures is limited to the number of crystallographically different pairs within the supercell. This method has been widely used in materials science to simulate defect-defect interactions in metals.[25–27] Here we show that it can be applied to simulate mixing and ordering in an isostructural solid solution, provided that certain conditions are fulfilled.

Although future applications will very likely be based on first-principles calculations, here we illustrate the method using a force-field model[28] which has been already successfully applied to simulate phase relations in the rhombohedral carbonates.[23] It has been shown[23] that the excess energies of various supercell structures in the calcite-magnesite system calculated with the potentials of Austen *et al.*[28] correlate linearly with the excess energies of the same structures calculated with a density-functional theory (DFT) based model.[10] The choice in favor of the force-field model allows comparison of the results with those obtained with the random sampling strategy.[23]

II. EXPANSION OF THE EXCESS ENTHALPY

The configurational energy of an $(A,B)R$ solid solution can be associated with interactions between the exchangeable (A,B) atoms only, while the interactions of A and B with the remainder of the structure R cancel out when the energy of the mechanical mixture of AR and BR end members is subtracted from the energy of the solid solution. Assuming pairwise additivity and extending the summation up to the nth distance within the supercell, the excess enthalpy can be written as

$$\Delta H = H_{\rm ss} - H_{\rm mm} = \frac{1}{2} N \sum_n Z_n \left(\sum_{i,j} P_{ij(n)} H_{ij(n)} - \sum_i P_i H_{ii(n)} \right), \tag{1}$$

where $H_{\rm ss}$ is the enthalpy of a solid solution phase with the composition $x_i = P_i$, $H_{\rm mm}$ is the enthalpy of the mechanical mixture of the end members, N is the number of the exchangeable sites in the supercell, $P_{ij(n)}$ is the probability of finding an ij pair at the nth distance in the supercell, $H_{ij(n)}$ is the interaction energy between atoms i and j, and Z_n is the coordination number (the number of neighbors at the nth distance). The enthalpy of the mechanical mixture is represented with AA and BB pairs only which occur with the probabilities (fractions) $P_{\rm A}$ and $P_{\rm B}$, respectively. Noting that the point probabilities P_i can be written as sums of the pair probabilities, $P_{\rm A} = P_{{\rm AB}(n)} + P_{{\rm AA}(n)}$ and $P_{\rm B} = P_{{\rm BA}(n)} + P_{{\rm BB}(n)}$, Eq. (1) can be rewritten as follows:

$$\Delta H = \frac{1}{2} N \sum_n Z_n P_{{\rm AB}(n)} J_n, \tag{2}$$

where

$$J_n = H_{{\rm AB}(n)} + H_{{\rm BA}(n)} - H_{{\rm AA}(n)} - H_{{\rm BB}(n)} \tag{3}$$

is the effective pair interaction at the distance n. It is convenient to rewrite Eq. (2) in the form

$$\Delta H = \sum_n f_{{\rm AB}(n)} J_n, \tag{4}$$

where $f_{{\rm AB}(n)}$ is one half of the number of AB pairs at the nth distance within the supercell.

This formula has been employed extensively in many recent studies of order/disorder and mixing phenomena in minerals.[14–24,29,30] The J's were calculated with the least-squares method from the static lattice energies and $f_{{\rm AB}(n)}$ numbers of a large set of supercell structures. Equation (4) was subsequently used to calculate temperature-dependent mixing properties with the Monte Carlo method. It has been recognized, however, that since the numbers of AB pairs are symmetric with respect to swapping A and B symbols, the predicted excess enthalpy is always a symmetric function with respect to $x=0.5$ as long as the J's are composition independent. Several studies[20,21,23,24] have shown that the accuracy of Eq. (4) for fitting the static lattice energies can be significantly improved by adding to Eq. (4) a configuration-independent term,

$$\Delta H_0 = x_1 x_2 (x_1 A_1 + x_2 A_2), \tag{5}$$

where x_i's are the mole fractions of the end members 1 and 2 and A_i's are parameters. The addition of this term is supported by the analysis of Ferreira *et al.*,[31] who showed that in

TABLE I. The numbers of Ca-Mg (AB) pairs, $f_{AB(n)}$, and the degeneracies D_n of the structures with single and double defects in the calcite-magnesite solid solution: $3\times3\times1$ supercell. L_n (Å) is the distance between the defects within the supercell.

n	L_n	$N_{def}:N_{host}$	$f_{AB(n)}$											D_n
			Single defects											
		1:53	3	3	3	3	3	6	1	3	6	6	6	
			Double defects											
1	4.052	2:52	**5**	6	6	6	6	12	2	6	12	12	12	1
2	4.994	2:52	6	**5**	6	6	6	12	2	6	12	12	12	1
3	6.382	2:52	6	6	**5**	6	6	12	2	6	12	12	12	1
4	6.431	2:52	6	6	6	**5**	6	12	2	6	12	12	12	1
5	8.104	2:52	6	6	6	6	**5**	12	2	6	12	12	12	1
6	8.142	2:52	6	6	6	6	6	**10**	2	6	12	12	12	2
7	8.541	2:52	6	6	6	6	6	12	**0**	6	12	12	12	2
8	8.650	2:52	6	6	6	6	6	12	2	**3**	12	12	12	3
9	9.519	2:52	6	6	6	6	6	12	2	6	**10**	12	12	2
10	9.893	2:52	6	6	6	6	6	12	2	6	12	**10**	12	2
11	12.156	2:52	6	6	6	6	6	12	2	6	12	12	**6**	6

solid solutions with size mismatch, ΔH_0 can be associated with the global strain that is caused by a homogeneous deformation of the lattices of the end members due to the mixing.

In a recent study of the calcite-magnesite system[23] the J and A parameters were determined by a least-squares method from the energies of about 800 randomly generated supercell structures. Although the experimental phase relations were successfully reproduced, the model[23] had several drawbacks. First, the set of the supercell structures was prepared by random swaps starting from the ordered compounds with a dolomite-type ordering pattern. This choice implied prior knowledge of the type of ordering in the system. Second, the A's and the J's were determined from the results of the least-squares fit. Within this procedure the separation of the configuration-dependent and -independent parts of the excess enthalpy cannot be done accurately because the symmetric part of the global strain overlaps with the J's expansion and thus the A_i parameters correlate severely with the values of the J's. The approach presented below avoids these inconveniences.

III. DOUBLE-DEFECT METHOD

It is easy to design a computational experiment which allows evaluation of the effective pair interaction at a given distance in the limit of infinite dilution. Let us consider AB, BA, AA, and BB pairs placed at the nth distance within the matrix of the pure "A" end member. In this case the differences in the enthalpies of the supercells of the same size containing AB, BA, AA, and BB pairs will be the same as the differences between $H_{AB(n)}$, $H_{BA(n)}$, $H_{AA(n)}$, and $H_{BB(n)}$ terms of Eq. (3). One can also note that the A atoms, which belong to the pairs, will be indistinguishable from the A atoms of the matrix. Hence, the AA pair will disappear, while the AB and BA pairs will reduce to single B-type defects within the A matrix. This means that in the diluted limit of the end member A, the J can be computed as the difference in total energies of sufficiently large supercells with single, double, and no B defects. Rescaling the enthalpies relative to the enthalpy of the supercell of pure A end member, one obtains

$$J_{A(n)} = 2\Delta H_B - \Delta H_{BB(n)}, \tag{6}$$

where $J_{A(n)}$ is the pair ECI at the distance n in the limit of pure A, and ΔH_B and $\Delta H_{BB(n)}$ are the excess enthalpies of the supercells with single B and double BB defects, respectively. Similarly, in the B limit

$$J_{B(n)} = 2\Delta H_A - \Delta H_{AA(n)}. \tag{7}$$

Equation (6) has been used to calculate interactions between impurity pairs in various metals and to predict solubility limits for various alloying components in metals.[25–27] Here we investigate the possibility of using this method to predict thermodynamic mixing behavior in a concentrated solid solution. Let us consider a $3\times3\times1$ supercell of $R\bar{3}c$ calcite ($a=14.964$ Å, $c=17.061$ Å) containing 54 exchangeable sites. The first two configurations are constructed from the pure end members by substituting one Ca in calcite with Mg and one Mg in magnesite with Ca. The other configurations are generated by adding a second defect at all possible distances around the first defect. This results in two series of configurations with Mg-Mg and Ca-Ca defects each comprising 11 structures, respectively. The enthalpies of the double-defect structures vary with the distance between the impurity atoms. Each of these structures is characterized with a unique set of numbers of AB (Ca-Mg) pairs. These numbers are given in Table I. An important feature of Table I is that nearly all numbers of AB pairs of the configurations with the double defects are equal to twice the corresponding numbers of the configurations with the single defect. This is

so because the number of dissimilar AB pairs generated by two defects is generally twice the number of AB's generated by a single defect. The only exceptions are the AB numbers which correspond to the distances at which the double defects are inserted. These "exceptional" numbers (the values in bold) occur along the diagonal direction of Table I. Due to the periodic boundary conditions, the insertion of a double defect generates D_n AA or BB pairs, where D_n is the degeneracy factor. The degeneracy is calculated by counting the number of symmetry-related pairs between the first defect and all translational variants of the second defect. Thus the exceptional AB numbers are smaller than twice the AB numbers of a single-defect structure by J_n times D_n. This means that in the case of periodic boundary conditions, Eq. (6) should be written as follows:

$$J_{A(n)} = (2\Delta H_B - \Delta H_{BB(n)})/D_n, \tag{8}$$

where D_n is the degeneracy.

The last equation and its analog for the B limit can be now used to calculate the J's in the calcite-magnesite system. To calculate the enthalpies of the single- and double-defect structures, we used the force-field model of Austen *et al.*[28] and the program GULP.[32,33] The excess enthalpies and the J's are given in Table II. The two sets of the J's correspond to the defects Mg(B) in calcite and the defects Ca(A) in magnesite.

The relationship between the excess enthalpies of the double-defect structures and the defect-defect distance is shown in Fig. 1. The excess enthalpies converge to a value which is close to twice the excess enthalpy of a single defect. Consequently, the J's converge with the defect separation to near zero value. This is consistent with the expectation that at a large distance the ordering interaction between two defects vanishes.

The two sets of the J's characterize the pair ECIs at two extremes along the composition axis. The variation in the J's at intermediate compositions is not known. However, in a system with size mismatch, referring to the analysis of Ferreira *et al.*,[31] one expects that the excess enthalpy in the high-temperature limit should be consistent with the subregular model, so that the total excess effect could be fitted with an equation similar to Eq. (4). Such a behavior is consistent with a linear dependence of the J's on the composition:

$$J_n = x_A J_{A(n)} + x_B J_{B(n)}. \tag{9}$$

Although alloy theories suggest more complex functional dependences of ECIs on the composition,[5,34] we think that the simplest assumption of a linear behavior could be sufficient in cases when the values of $J_{A(n)}$ and $J_{B(n)}$ are very similar. This is indeed the case for the calcite-magnesite solid solution (Fig. 2).

IV. PRACTICAL IMPLEMENTATION OF THE DDM

The derivation given above suggests that the J's calculated with Eqs. (8) and (9) after substitution into Eq. (4) should reproduce the excess enthalpies of the double and single defects. In contrast to this expectation such a test shows that the recalculated excess enthalpies differ considerably from the initial ones, which have been calculated directly from the force-field model. However, we note that when the single-defect enthalpy in Eq. (8) is allowed to deviate from the computed value and is treated as a fitting parameter instead, nearly perfect agreement with the initial enthalpies is achieved easily. Therefore, this test suggests that the enthalpies of the double-defect structures converge to a value, which is very close, but not exactly equal, to twice the enthalpy of a single-defect structure. It is clear that the enthalpies of the double-defect structures converge to the enthalpy of a structure with two noninteracting defects. Such a hypothetic structure should have the same composition as the other double-defect structures, i.e., two defects per supercell. Equation (8) assumes that the excess enthalpy of this structure is equal to twice the excess enthalpy of the structure with a single defect. Although this is correct in the case of an infinitely large supercell (Henry's law), practically, we are dealing with rather small supercells, in which the excess enthalpy is not linearly proportional to the composition. Therefore, Eq. (8) is slightly inaccurate. In order to achieve the consistency, the enthalpy of the single-defect structure should be adjusted so that twice this value gives the enthalpy of a hypothetical structure with two noninteracting defects. Following this idea the DDM recipe is reformulated as follows:

$$J_{A(n)} = (\Delta H_{BB(\infty)} - \Delta H_{BB(n)})/D_n, \tag{10}$$

where $\Delta H_{BB(\infty)}$ is a single parameter for all the J's corresponding to defects of BB type. When the J's are calculated at two contrasting compositions (in the A and B limits), two parameters are needed. These parameters can be found by substituting the J's calculated with Eq. (10) into Eqs. (9) and (4) and by fitting to the known excess enthalpies and $f_{AB(n)}$ numbers of the single- and double-defect structures. The fitted $\Delta H_{BB(\infty)}$ and $\Delta H_{AA(\infty)}$ values together with the corresponding values of the J's are listed in column 7 of Table II and plotted in Fig. 2. The comparison of columns 4 and 5 of Table II shows that the excess enthalpies of double-defect structures can be fitted very accurately using these two adjustable parameters. It is important to note that Eq. (10) can be applied not only to the excess enthalpies of double-defect structures, but also to their absolute enthalpies. The meaning and the value of the adjustable parameter will change accordingly. Its optimized value will be then close to twice the absolute enthalpy of a single-defect structure.

V. ENTHALPY IN THE HIGH-TEMPERATURE LIMIT

When the J's are known, the enthalpy of mixing in the high-temperature limit can be straightforwardly calculated with Eq. (2). Since the atomic distribution is purely random, the probabilities of AB pairs in Eq. (2) can be substituted with the product $P_A P_B = P_A(1-P_A)$. Since the J's vary with composition, the high-temperature enthalpy is asymmetric with respect to $x=0.5$. This asymmetric function can be visualized as a linear interpolation between two symmetric functions of different amplitudes which result from using

TABLE II. The excess enthalpies of the single- and double-defect structures and the pair ECIs in the calcite-magnesite solid solution: $3\times3\times1$ supercell. The enthalpy values are in eV. The fitted values are marked with the $*$ sign. The values in bold are the excess enthalpies of the hypothetical compounds with the defects at an infinitely large distance.

Single defects

$N_B:N_A$	$\Delta H_{A/B}$	$\Delta H^*_{A/B}$
1:53	0.2217	0.2204
53:1	0.3451	0.3441

Double defects

n	L_n (Å)	$N_B:N_A$	$\Delta H_{BB(n)}$	$\Delta H^*_{BB(n)}$	$J_{A(n)}$	$J^*_{A(n)}$
1	4.052	2:52	0.5675	0.5663	−0.1242	−0.1219
2	4.994	2:52	0.3581	0.3574	0.0853	0.0875
3	6.382	2:52	0.4279	0.4279	0.0154	0.01770
4	6.431	2:52	0.4459	0.4457	−0.0025	−0.0002
5	8.104	2:52	0.3977	0.3981	0.0456	0.0479
6	8.142	2:52	0.3780	0.3783	0.0327	0.0338
7	8.541	2:52	0.3791	0.3812	0.0321	0.0333
8	8.650	2:52	0.4640	0.4640	−0.0069	−0.0061
9	9.519	2:52	0.4826	0.4820	−0.0196	−0.0185
10	9.893	2:52	0.4267	0.4268	0.0083	0.0095
11	12.156	2:52	0.4848	0.4838	−0.0069	−0.0065
∞		2:52		**0.4456**	0	0

n	L_n (Å)	$N_B:N_A$	$\Delta H_{AA(n)}$	$\Delta H^*_{AA(n)}$	$J_{B(n)}$	$J^*_{B(n)}$
1	4.052	52:2	0.7733	0.7745	−0.0832	−0.0898
2	4.994	52:2	0.5779	0.5786	0.1123	0.1056
3	6.382	52:2	0.6670	0.6670	0.0231	0.0164
4	6.431	52:2	0.6798	0.6799	0.0104	0.0037
5	8.104	52:2	0.6470	0.6466	0.0431	0.0364
6	8.142	52:2	0.6260	0.6257	0.0320	0.0287
7	8.541	52:2	0.6735	0.6714	0.0083	0.0050
8	8.650	52:2	0.7029	0.7029	−0.0043	−0.0065
9	9.519	52:2	0.7050	0.7057	−0.0075	−0.0108
10	9.893	52:2	0.6668	0.6668	0.0116	0.0083
11	12.156	52:2	0.6972	0.6982	−0.0012	−0.0023
∞		52:2		**0.6835**	0	0

$J_{A(n)}$ or $J_{B(n)}$ (Fig. 3). One observes that the high-temperature enthalpy passes nearly exactly through the excess enthalpies of the two structures with single defects. This is not a coincidence. The probability of finding an AB pair in a structure with a single A defect is $P_A P_{B/A}=P_A$. This holds because the conditional probability $P_{B/A}$ (the probability of finding B atom at a given distance from an A atom) is equal to 1. Since in the diluted composition limit

$$P_A(1-P_A)\approx P_A, \tag{11}$$

the high-temperature enthalpy is bound to pass almost exactly through the excess enthalpy of the single-defect structure. Thus, as it was already shown by Sluiter and Kawazoe,[35] the high-temperature enthalpy can be predicted from the excess enthalpies of just two single defects. The predicted type of asymmetry with the maximum shifted to magnesite-rich compositions is consistent with the shape of the phase diagram of the calcite-magnesite system,[36] which shows that the miscibility gap at magnesite-rich compositions is wider than the gap at calcite-rich compositions.

VI. MONTE CARLO SIMULATIONS

Fast convergence of the ECIs as a function of interatomic separation (Fig. 2) suggests that Eq. (4) is applicable for

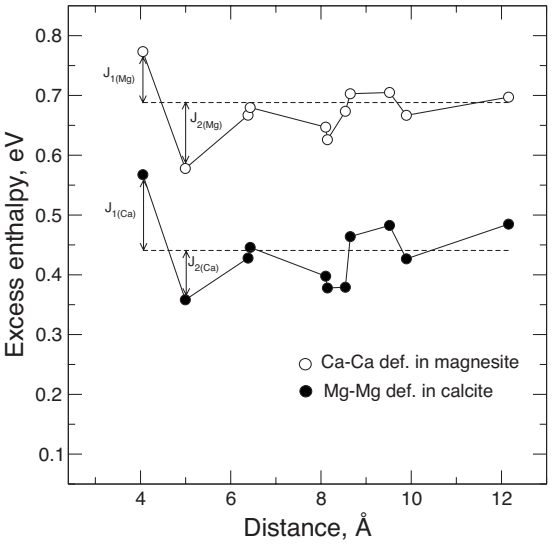

FIG. 1. The excess enthalpies of double-defect structures. White and black circles correspond to Ca-Ca defects in magnesite and Mg-Mg defects in calcite, respectively. The dashed lines show twice the excess enthalpy of the structures with the single Mg or Ca defects. Arrows show the magnitude of the J's.

calculation of excess enthalpies in a much larger supercell. Here we employ a $12\times12\times3$ supercell which contains 2592 exchangeable atoms. The previous study[23] has shown that supercells of this size already approach the thermodynamic limit. It has been shown that the thermodynamic averages calculated for $12\times12\times3$ and $16\times16\times4$ supercells are practically indistinguishable. Canonical Monte Carlo simulations were performed with the composition-dependent J's on a grid of 54 compositions between calcite and magnesite and 21 temperatures between 500 and 2500 K. To achieve equilibrium 15×10^9 Monte Carlo steps were used and another 15×10^9 steps were used to calculate averages. The results of the simulations are shown in Fig. 4.

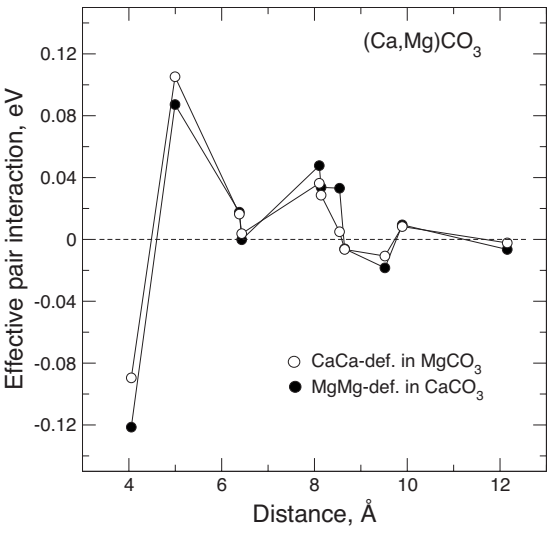

FIG. 2. The effective pair interactions, the J's, in rhombohedral carbonates predicted with the double-defect method (DDM). The values of the J's are given in the last column of Table I.

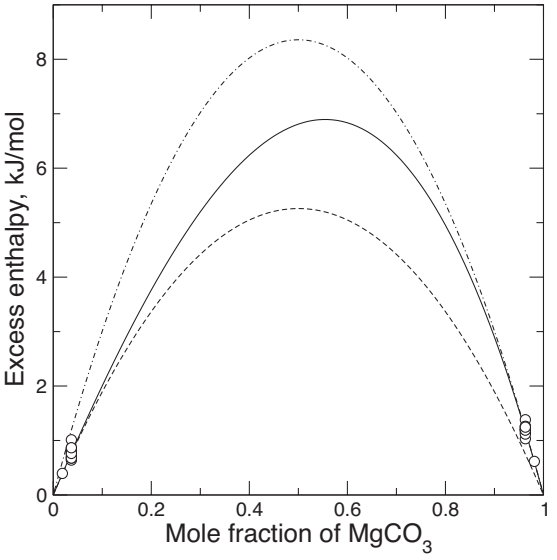

FIG. 3. The enthalpies of mixing in the calcite-magnesite system in the high-temperature limit. The dot-dashed and dashed lines show the enthalpies predicted from Ca-Ca defects in magnesite and Mg-Mg defects in calcite, respectively. Circles show the excess enthalpies of the single- and double-defect structures in kJ/mol assuming the formula unit with one exchangeable atom. The solid line is the interpolation using Eq. (8).

VII. THERMODYNAMIC INTEGRATION

The configurational free energy can be calculated from Monte-Carlo-averaged excess enthalpies via a λ integration:[37,38]

$$\Delta G = \Delta G_0 + \int_0^1 \Delta H_\lambda d\lambda . \tag{12}$$

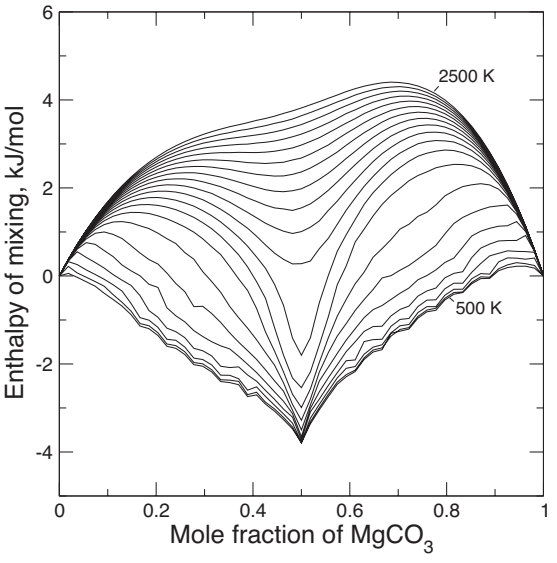

FIG. 4. The enthalpy of mixing as a function of temperature from Monte Carlo simulations. The values are in kJ/mol assuming a formula unit with one exchangeable atom.

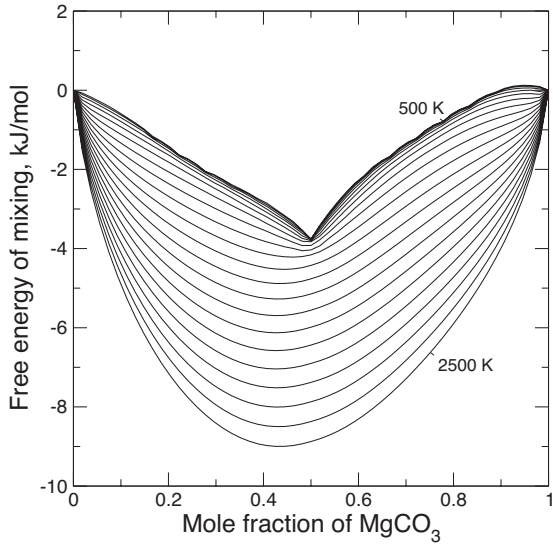

FIG. 5. The free energies of mixing calculated with the thermodynamic integration method.

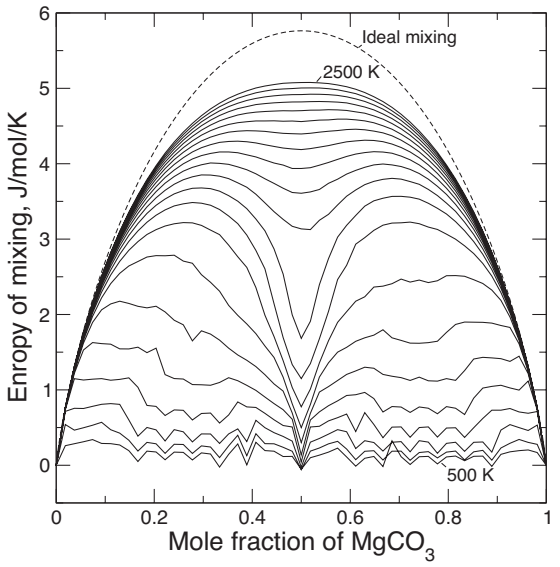

FIG. 6. Configurational entropy isotherms derived from the simulated enthalpies and free energies of mixing using Eq. (14).

ΔG_0 is the free energy of mixing of an $(A,B)R$ solid solution with completely random distribution of A and B atoms, which can be calculated theoretically:

$$\Delta G_0 = \Delta H_0 + RT[x_A \ln(x_A) + x_B \ln(x_B)], \tag{13}$$

where ΔH_0 is the enthalpy of mixing in the limit of complete disorder and ΔH_λ is the average enthalpy of the system in a state with a nonequilibrium intermediate degree of chemical disorder, λ; $0<\lambda<1$. The state $\lambda=1$ corresponds to an equilibrated system at a given temperature, while the states with $\lambda<1$ correspond to an artificial disorder that is introduced on top of the equilibrium disorder at the same temperature. This artificial disorder is simulated by scaling the J's according to the equation $J_n^\lambda=\lambda J_n$. In our simulations, λ was gradually increased from 0 to 1 with a step size of 0.04. The integral describes the change in free energy of a system at a fixed temperature from the state with zero ordering energy ($\lambda=0$) to its equilibrium state determined with the nominal values of the J's ($\lambda=1$). The free-energy isotherms are plotted in Fig. 5. Configurational entropy isotherms were calculated with

$$\Delta S = (\Delta H - \Delta G)/T \tag{14}$$

and are plotted in Fig. 6. The remarkable feature of the low-temperature isotherms is the sharp minimum at $x=0.5$ that is caused by dolomite-type ordering. The temperature dependence of the long-range-order (LRO) parameter at $x=0.5$ has been investigated with the Monte Carlo simulation (Fig. 7). The LRO parameter is defined as

$$Q = (P_{A\alpha} - P_{A\beta})/(P_{A\alpha} + P_{A\beta}), \tag{15}$$

where $P_{A\alpha}=P_A(1+Q)$ and $P_{A\beta}=P_A(1-Q)$ are the probabilities of finding an A (Ca) atom in the nonequivalent sublattices α and β of the dolomite structure. Equation (15) cannot be directly applied for calculating the order parameter. The problem is that the ordering pattern fluctuates from Q to $-Q$ during the simulation. Thus the site occupancies calculated over a long simulation run are equal to the concentration of A in the Monte Carlo supercell. Therefore, the value of Q at a given temperature was evaluated from the probability (occurrence frequency) of A-A pairs at the maximum separation (25.59 Å along the c axis) permitted by $12\times12\times3$ supercell. Since short-range order at such a large distance is practically absent, the probability of A-A (Ca-Ca) pairs can be evaluated as the product of the instantaneous occurrence frequencies of A (Ca) within the sublattices:

$$P_{AA} \approx P_{A\alpha}P_{A\beta} = P_A^2(1-Q^2), \tag{16}$$

where $P_A=0.5$. The temperature of the order/disorder $R\bar{3}c/R\bar{3}$ transition of 1475 ± 25 K is close to the experimental value[39] of 1398 ± 25 K.

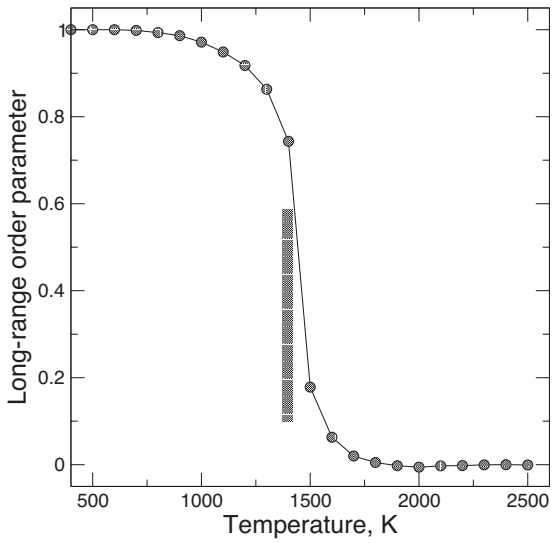

FIG. 7. The temperature dependence of the long-range-order parameter. Circles—the results of the present Monte Carlo simulations. The width of the shaded rectangle shows the estimated uncertainty of the experimental value of the transition temperature (Ref. 39).

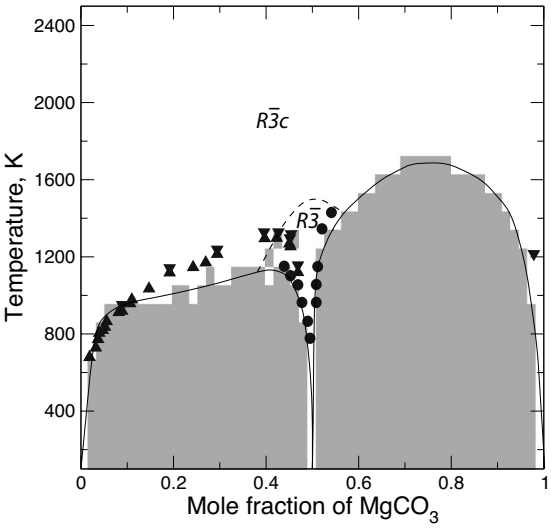

FIG. 8. Phase relations in the calcite-magnesite system. Shaded boxes—the unstable compositions selected based on the common tangent analysis of the free-energy isotherms. Solid lines—the guide-to-the-eye phase boundaries. The dashed line encircles the field of stability of the dolomite phase (see text). The symbols are the equilibrium compositions from the experimental study of Goldsmith and Heard (Ref. 40).

VIII. PHASE DIAGRAM

The free energies of mixing were converted to a phase diagram by comparing the free energy at each composition x_i along an isotherm to the free energy of a mechanical mixture x_j+x_k. If there is a pair of compositions x_j+x_k that has lower free energy, the solution with composition x_i is unstable or metastable. The two miscibility gaps were thus outlined. The predicted shape of the phase diagram (Fig. 8) is the consequence of the large negative excess enthalpy of the ordered intermediate compound $R\bar{3}$, dolomite. The predicted excess enthalpy of −3.79 kJ/mol is in good agreement with the experimental value,[41] -5.74 ± 0.25 kJ/mol, and with the result of a DFT calculation using the VASP code, −3.66 kJ/mol.[10] The calculated phase relations are in good agreement with the experimental data.[40,42]

IX. DISCUSSION AND CONCLUSIONS

The predicted phase relations in the calcite-magnesite system are very much consistent with those obtained in the previous simulation study[23] based on the random sampling approach. This shows that the DDM is able to produce results of comparable accuracy by sampling a much smaller set of the supercell structures. Moreover, the intermediate dolomite phase is predicted without any preliminary knowledge of the type of ordering in the system. The correct asymmetry of phase diagram is modeled solely based on the predicted pairwise interactions, without an addition of a configuration-independent term. This means that the pairwise interactions, which are responsible for ordering at intermediate compositions, can be, in fact, predicted from the excess enthalpies of the structures whose compositions approach the diluted limits. Therefore, in cases where the interatomic interactions are well described with the pairwise terms, the sampling of the intermediate composition range is not necessary. Since the structures with the double defects can be easily enumerated and since the number of such structures is very limited, there appears the possibility of predicting mixing properties of isostructural solid solutions solely on the basis of first-principles calculations. The method appears to be especially attractive for systems such as garnets, where the unit cell is intrinsically large due to the presence of extra elements not involved in mixing. The DDM permits then to select the minimum number of the basis structures needed for the development of the model of mixing.

The DDM approach is based on the assumption that many-body interactions can be ignored. This condition seems to be fulfilled in solid solutions in which interatomic interactions are mediated by extra inactive structural units such as CO_3^{2-} in carbonates and SiO_4^{4-} in silicates. The common experience of mineralogists suggests that interatomic interactions in such systems can be accurately described with centrally symmetric cation-anion and angle-dependent cation-anion-cation potentials.[43–45] The specific cation-cation interactions are modeled as purely electrostatic. Thus it is not surprising that the pairwise ECI are sufficient for the description of the cation order in the carbonates. However, the DDM might not work in alloys, where many-body interactions cannot be neglected.[46] For example, the study of Asato *et al.*[27] showed that the prediction of solubility limits in Rd-Pd alloy is significantly improved when three- and four-body interactions are taken into account. In such cases the double-defect approach could be extended to include triple or quadruple defects as it was outlined by Asato *et al.*[27] The number of such structures rapidly increases with the system size, however.

ACKNOWLEDGMENTS

V.L.V. gratefully acknowledges research funding from the Deutsche Forschungsgemeinschaft (Grant No. WI 1232/27-1) and from the Helmholtz Society (The Virtual Institute for Advanced Solid-Aqueous Radio-Geochemistry). We also wish to thank J. D. Gale, N. Paulsen, and D. J. Wilson for the help with calculations.

*v.vinograd@kristall.uni-frankfurt.de

[1] J. W. D. Connolly and A. R. Williams, Phys. Rev. B **27**, 5169 (1983).
[2] A. Zunger, in *Statics and Dynamics of Alloy Phase Transformations*, edited by P. Turchi and A. Gonis (Birkhäuser, 1994), pp. 361–419.
[3] D. de Fontaine, Solid State Phys. **47**, 33 (1994).
[4] L. G. Ferreira, S. H. Wei, and A. Zunger, Phys. Rev. B **40**, 3197 (1989).
[5] M. Sluiter, D. de Fontaine, X. Q. Guo, R. Podloucky, and A. J. Freeman, Phys. Rev. B **42**, 10460 (1990).
[6] S. H. Wei, L. G. Ferreira, and A. Zunger, Phys. Rev. B **41**, 8240 (1990).
[7] M. Asta, D. de Fontaine, M. van Schilfgaarde, M. Sluiter, and M. Methfessel, Phys. Rev. B **46**, 5055 (1992).
[8] C. Wolverton and A. Zunger, Comput. Mater. Sci. **8**, 107 (1997).
[9] M. H. F. Sluiter, C. Colinet, and A. Pasturel, Phys. Rev. B **73**, 174204 (2006).
[10] B. Burton and A. van de Walle, Phys. Chem. Miner. **30**, 88 (2003).
[11] B. Burton and A. van de Walle, Chem. Geol. **225**, 222 (2006).
[12] B. Burton, A. van de Walle, and U. Kattner, J. Appl. Phys. **100**, 113528 (2006).
[13] A. van de Walle and G. Ceder, J. Phase Equilib. **23**, 348 (2002).
[14] A. Bosenick, M. Dove, and C. Geiger, Phys. Chem. Miner. **27**, 398 (2000).
[15] U. Becker, A. Fernandez-Gonzalez, M. Prieto, R. Harrison, and A. Putnis, Phys. Chem. Miner. **27**, 291 (2000).
[16] U. Becker and K. Pollock, Phys. Chem. Miner. **29**, 52 (2002).
[17] M. Warren, M. Dove, E. Myers, A. Bosenick, E. Palin, C. Sainz-Diaz, and B. Guiton, Miner. Mag. **65**, 221 (2001).
[18] E. Palin and R. Harrison, Am. Mineral. **92**, 1334 (2007).
[19] J. Purton, N. Allan, M. Lavrentiev, I. Todorov, and C. Freeman, Chem. Geol. **225**, 176 (2006).
[20] V. Vinograd, M. Sluiter, B. Winkler, A. Putnis, U. Hålenius, J. Gale, and U. Becker, Miner. Mag. **68**, 101 (2004).
[21] V. Vinograd and M. Sluiter, Am. Mineral. **91**, 1815 (2006).
[22] V. Vinograd, B. Winkler, A. Putnis, H. Kroll, V. Milman, J. Gale, and O. Fabrichnaya, Mol. Simul. **32**, 85 (2006).
[23] V. Vinograd, B. Burton, J. Gale, N. Allan, and B. Winkler, Geochim. Cosmochim. Acta **225**, 304 (2007).
[24] V. Vinograd, B. Winkler, and J. Gale, Phys. Chem. Miner. **34**, 713 (2007).
[25] T. Hoshino, W. Schweika, R. Zeller, and P. H. Dederichs, Phys. Rev. B **47**, 5106 (1993).
[26] T. Hoshino, R. Zeller, and P. H. Dederichs, Phys. Rev. B **53**, 8971 (1996).
[27] M. Asato, T. Hoshino, and K. Masuda-Jindo, J. Magn. Magn. Mater. **226-230**, 1051 (2001).
[28] K. Austen, K. Wright, B. Slater, and J. Gale, Phys. Chem. Chem. Phys. **7**, 4150 (2005).
[29] M. Dove, in *Microscopic Properties and Processes in Minerals*, NATO Advanced Studies Institute, Series C: Mathematical and Physical Sciences, edited by K. Wright and R. Catlow (Kluwer, Dordrecht, 1999), Vol. 543, pp. 451–475.
[30] A. Bosenick, M. Dove, E. Myers, E. Palin, C. Sainz-Diaz, B. Guiton, M. Warren, M. Craig, and S. Redfern, Miner. Mag. **65**, 193 (2001).
[31] L. G. Ferreira, A. A. Mbaye, and A. Zunger, Phys. Rev. B **37**, 10547 (1988).
[32] J. Gale, J. Chem. Soc., Faraday Trans. **93**, 629 (1997).
[33] J. Gale and A. Rohl, Mol. Simul. **29**, 291 (2003).
[34] P. Turchi, M. Sluiter, and D. de Fontaine, Phys. Rev. B **36**, 3161 (1987).
[35] M. Sluiter and Y. Kawazoe, Europhys. Lett. **57**, 526 (2002).
[36] J. Goldsmith and H. Heard, J. Geol. **69**, 45 (1961).
[37] E. Myers, V. Heine, and M. Dove, Phys. Chem. Miner. **25**, 457 (1998).
[38] M. Dove, in *Solid Solution in Silicate and Oxide Systems*, EMU Notes in Mineralogy Vol. 3, edited by C. Geiger (Eötvös University Press, Budapest, 2001), pp. 225–249.
[39] R. J. Reeder and Y. Nakajiuma, Phys. Chem. Miner. **8**, 29 (1982).
[40] J. Goldsmith and H. Heard, J. Geol. **80**, 611 (1961).
[41] A. Navrotsky and C. Capobianco, Am. Mineral. **72**, 782 (1987).
[42] J. Goldsmith, Rev. Mineral. **11**, 49 (1983).
[43] M. J. Sanders, M. Leslie, and C. R. A. Catlow, J. Chem. Soc., Chem. Commun. **1984**, 1271.
[44] B. Winkler, M. T. Dove, and M. Leslie, Am. Mineral. **76**, 313 (1991).
[45] J. D. Gale, Philos. Mag. B **73**, 3 (1996).
[46] A. V. Ruban and I. A. Abrikosov, Rep. Prog. Phys. **71**, 046501 (2008).